Carbohydrate Polymers 86 (2011) 1586–1594

Contents lists available at ScienceDirect

Carbohydrate Polymers

journal homepage: www.elsevier.com/locate/carbpol

Surface functionalisation of cellulose with noble metals nanoparticles through a selective nucleation

Sami Boufi[a], Ana Maria Ferraria[b], Ana Maria Botelho do Rego[b,*], Nicolas Battaglini[c], Frédéric Herbst[c], Manuel Rei Vilar[c]

[a] Laboratoire des Sciences des Matériaux et Environnement, Faculté des Sciences de Sfax, University of Sfax, Tunisia
[b] Centro de Química-Física Molecular and Institute of Nanoscience and Nanotechnology, IST, Technical University of Lisbon, Portugal
[c] Univ. Paris Diderot, Sorbonne Paris Cité, ITODYS, UMR 7086 CNRS, 75013, Paris, France

ARTICLE INFO

Article history:
Received 24 May 2011
Received in revised form 21 June 2011
Accepted 23 June 2011
Available online 1 July 2011

Keywords:
Cellulose
Silver
Gold
Nanoparticles
Film
Surface

ABSTRACT

Films and fibres of cellulose were functionalised with silver and gold nanoparticles directly generated on the surface. The present method lays on the cellulose surface pre-modification, replacing some of the hydroxyl groups by amino functions, which selectively act as the seed coordination sites. Nanoparticles can then grow through the interaction with aqueous dilute solutions of $AgNO_3$ or $NaAuCl_4$ at room temperature, without adding any reducing agent. The procedure offers the advantage of limiting the generation of nanoparticles to the cellulose surface, leaving the dispersion medium completely exempt of them. The cellulose pre-modification also ensures chemical anchoring of the nanoparticles to the surface, avoiding any risk of particle desorption and extending the lifetime of the resulting hybrid materials. Evidence of the formation of the NPs on the cellulose surfaces was supported by FE-SEM, AFM, XPS and XRD. The method is simple and reproducible.

1. Introduction

Metallic nanoparticles have been the focus of intensive research in the past decades and opened the way toward the preparation of advanced functional materials having applications in different areas including electronics (Maier et al., 2001), namely sensing devices with novel functionalities, catalysis (Campbell, Parker, & Starr, 2002), and biomedicine (Daniel & Astruc, 2004). Developing methods for immobilizing such nanoparticles onto surfaces will be very useful for many of these applications. Of particular significance are electrically conducting substrates, optical sensing devices and specific membranes. Several approaches have been developed for the immobilisation of metal NPs on a variety of substrates, such as dendrimers (Esumi, Isono, & Yoshimura, 2004; Scott, Wilson, & Crooks, 2005), latex particles (Agrawal et al., 2007; Agrawal, Pich, Zafeiropoulos, & Stamm, 2008), and microgels (Malynych, Luzinov, & Chumanov, 2002; Pich et al., 2005; Rubio-Retama et al., 2007). Very recently, platinum nanoparticles have been synthesised on cellulose using reducing agents (Benaissi, Johnson, Walsh, & Thielemans, 2010). In this work, we introduce a simple, reproducible and economic method to grow metal NPs directly on cellulose substrates.

The use of cellulose, either as a reductant or stabiliser, in the synthesis of NPs was the subject of several studies. Silver, gold, and platinum nanoparticles were synthesised through hydrothermal reduction by cellulose (transparent nanoporous cellulose gel was used as supporting medium) or by adding a reductant (Cai, Kimura, Wada, & Kuga, 2009). Silver NPs were deposited on the surface of cellulose microfibrils, previously oxidised by periodate (Wu, Kuga, & Huang, 2008). In another study, silver NPs were prepared with carboxymethyl cellulose sodium that effectively works as both reducing and stabilizing reagent (Chen, Wang, Zhang, & Jin, 2008). Actually, the porous texture, characteristic of cellulose matrix and fibres, has been found to work as a template for metal nanosized particles and has been shown to be a useful support material for different metal nanoparticles of platinum, palladium, silver, and copper (He, Kunitake, & Nakao, 2003; Vainio et al., 2007). Among the metal NPs, silver and gold have been the most studied mainly due to the well-known wide range of applications. The antibacterial activity of silver is being explored commercially in applications such as antibacterial textiles, to prevent infections and to treat burn injuries (Taylor, Ussher, & Burrel, 2005). Immobilisation of Ag nanoparticles on bacterial cellulose fibrils was achieved using triethanolamine as chelating-reducing agent (Barud et al., 2008). Silver nanoparticles impregnated into bacterial cellulose, using

---

* Corresponding author at: CQFM and IN, Instituto Superior Técnico, Av. Rovisco Pais, n°1, 1049-001 Lisboa, Portugal. Tel.: +351 218419255/7; fax: +351 218464455.
E-mail address: amrego@ist.utl.pt (A.M.B. do Rego).

0144-8617/$ – see front matter © 2011 Elsevier Ltd. All rights reserved.
doi:10.1016/j.carbpol.2011.06.067

different reducing agents, were prepared by immersing bacterial cellulose in a silver nitrate solution (Maria et al., 2009). Cellulose filter paper grafted with acrylamide followed by entrapment of silver nanoparticles results in development of a biomaterial with a fair biocidal action against, for instance, *Escherichia coli*. It can be also used as an antibacterial packaging material to prevent food stuff from bacterial infection (Tankhiwale & Bajpai, 2009). Gold NPs have multiple applications namely in domains as electronics and catalysis or for biomedical applications including labelling, drug delivery, heating and sensing (Sperling, Gil, Zhang, Zanella, & Parak, 2008).

In a previous work, we have shown that selective growth of Ag NPs could be generated on an amine modified cellulose film using, for this purpose, DMSO as a reducing agent. The cellulose films are an excellent model to study the NPs production in heterogeneous phase. Now, we extend our investigation toward a simpler, more economical and ecological method using aqueous solutions, as precursors, without the need of DMSO. The NPs could be selectively generated on the cellulose surface thanks to the presence of amino groups appended on the surface and acting as nucleating sites, and the hydroxyl groups of the anhydroglucosic unit (AGU) of the cellulose acting as reducing agents. For selective implantation of the nanoparticles, the prerequisite step consists always on the modification of the cellulose film surface through a derivatisation with di- or triaminoalkanes (Ferraria, Boufi, Battaglini, Botelho do Rego, & Vilar, 2010). In this case, one of the amine functions, or even two, in the case of the triamine, acts as an anchoring group to the carbonyldiimidazol activated cellulose film through a carbamate linkage. The remaining terminal amine groups stay available for further reaction, which, in this case, is the nucleation of silver or gold nanoobjects. This can be applied either on films, or even on fibres or other cellulosic materials.

The potentialities of the applications and the interesting science associated to the surface chemistry of the most abundant polymer on Earth, led us to investigate the possibility of grafting silver and gold NPs on its surface. The build-up of these hybrid materials, where NPs are chemically linked to cellulose may be particularly useful in different fields, as referred above, namely in the production of innovative products in paper and textile engineering. Comparatively to other methods, this one achieves undoubtedly, a higher resistant attachment of the NPs to the cellulosic substrates and assures longer lifetimes to the material. Moreover, it employs methods obeying the “green chemistry twelve principles” (http://www.epa.gov/greenchemistry/).

2. Material and methods

2.1. Materials

Semi-insulating single crystal GaAs (1 0 0) wafers were acquired from Geo Semiconductors Ltd. Anhydrous dimethylsulphoxide (DMSO) 99.7% was received from Acros Organic and tetrahydrofurane (THF), analytical reagent, from Riedel De Haën. N,N′-Carbonyldiimidazole (CDI), 1,4-diaminobutane (DAB) and 1,6-diaminohexane (DAH) and tris(2-aminoethyl)amine (TAEA) were purchased from Aldrich. Hydrochloric acid (37%) was received from J.T. Baker. Deionised water with a resistivity of 18.2 MΩ cm was supplied by a Millipore system (Simplicity) fed with distilled water. Avicel fibres were provided by Aldrich. Silver nitrate and sodium tetrachloroaurate (III) dihydrate were provided by Alfa Aesar with purity higher than 99% and 99.99%, respectively.

2.2. Sample preparation

A solution of cellulose in anhydrous DMAC/LiCl was prepared as described elsewhere (Vilar, Boufi, Ferraria, & Botelho do Rego, 2007). A part of this first solution was used to derivatise cellulose to obtain the trimethylsilylcellulose (TMSC) needed to obtain films cast on clean GaAs (1 0 0) or glass surface by spin-coating. Cellulose films (Cell-R) were obtained by exposing the TMSC films to hydrochloric acid vapours for 30 s, exchanging the trimethylsilyl groups by hydroxyl ones following a procedure already described (Boufi, Rei Vilar, Parra, Ferraria, & Botelho do Rego, 2008). The other part of the first solution was used to prepare the cellulose amine-derivatised solution. To derivatise the cellulose in all types of samples with amine groups, the cellulose alcohol groups were first activated with CDI and then reacted with DAB, DAH, or TAEA following a procedure described before for film derivatisation. To obtain the amine derivatised fibres, the following protocol was used: CDI was added to the first solution in a proportion 2 times the equivalent number of hydroglucosic units (AGU) and the solution was kept under stirring at 50 °C for 3 h, followed by the addition of one of the above cited amines (1.5 times the equivalent number of AGU). After stirring for 6 h, at room temperature, the derivatised cellulose was obtained by precipitation in a mixture of methanol/water followed by centrifugation. The structure of the amine-derivatised cellulose is presented in Scheme 1.

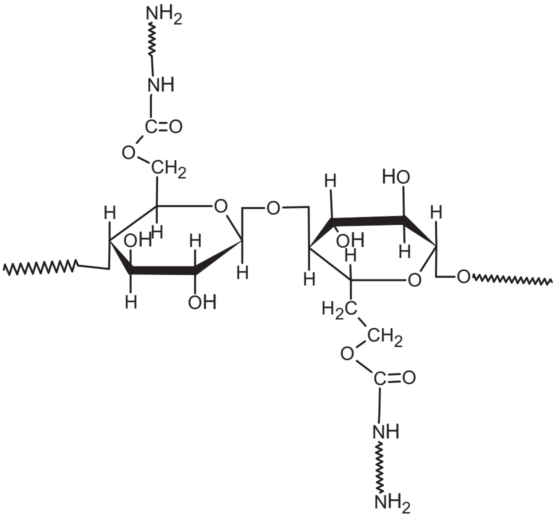

Scheme 1. cellulose derivatised with amino groups.

Films of both Cell-R and amine-derivatised Cell-R were immersed for different times in an aqueous solution of $AgNO_3$ (5×10^{-3} M) and then exhaustively washed with deionised water to strip off any physisorbed species.

The procedure for the surface modification of the fibres with amino groups was carried according to the procedure described by Alila, Ferraria, Botelho do Rego, & Boufi (2010): the fibres were introduced in a three neck flask containing a mixture of toluene/DMF (60/40, v/v), equipped with a Dean-Stark system, and kept under reflux until all the residual water retained by the fibres had been removed by azeotropic distillation. The suspension was then cooled to 60 °C, and CDI was added under dry nitrogen atmosphere and kept under magnetic stirring for 3 h. Next, the reaction mixture was rapidly filtered and washed twice with dry toluene in order to eliminate all the residual CDI. The activated fibres were then introduced in a three-neck flask containing a solution of the diamine (concentration about 10^{-3} mol L^{-1}), and kept under magnetic stirring and dry nitrogen atmosphere at 60 °C for 3 h. Finally, the recovered product was purified by Soxhlet extraction with toluene for 24 h, and dried at 40 °C.

To generate NPs on the modified fibres, a procedure analogous to the one used for films was applied, starting with the immersion of the modified fibres in aqueous solutions, of either $AgNO_3$

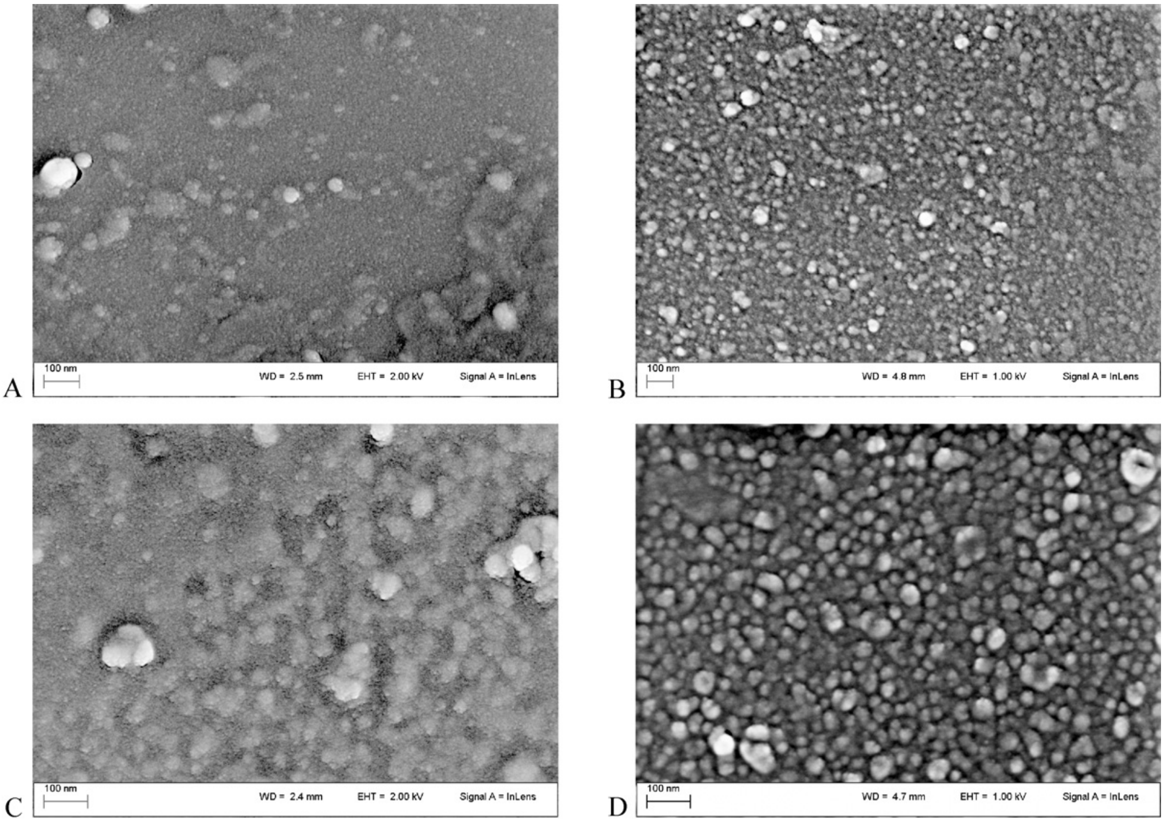

Fig. 1. FE-SEM images of an amine-functionalised cellulose film deposited on a glass plate after interaction with: (A) the $AgNO_3$ solution at room temperature for 15 min; (B) the $AgNO_3$ solution at room temperature for 45 min; (C) the $NaAuCl_4$ solution at 70 °C for 15 min; (D) a $NaAuCl_4$ solution at 70 °C for 45 min.

or $NaAuCl_4$ for different contact times. With $AgNO_3$ solution, the suspension was kept under magnetic stirring at room temperature, whereas with $NaAuCl_4$, the temperature was maintained at 70 °C.

2.3. Characterisation methods

An APT spin coating apparatus was used for the deposition of the trimethylsilylcellulose (TMSC) films. XPS spectra were recorded using Mg Kα and Al Kα radiation ($h\nu = 1253.6$ eV and 1486.6 eV, respectively) from an XSAM800 (KRATOS) XPS dual anode spectrometer. Spectra acquisition conditions and data treatment details were reported elsewhere (Ferraria, Lopes da Silva, & Botelho do Rego, 2003). Freeware XPS Peak 4.1 was used for fittings. Multimode Scanning Probe Microscope set-up driven by the Nanoscope IIIa electronics, from Digital Instruments, was used to obtain AFM images in the intermittent contact mode at room conditions. WSxM software was used to analyze and process data (Horcas et al., 2007). Absorption spectra in the ultraviolet and visible wavelength range (UV/vis) were recorded with a Cary-Varian spectrophotometer. Field Emission Scanning Electron Microscope (FE-SEM) images were obtained with a ZEISS SUPRA40, which is completely controlled from a computer workstation. The electron source, a hot cathode producing electrons by Schottky effect, is a tungsten filament coated with a ZrO layer. Images were processed using the software SMARTSEM. X-ray diffraction (XRD) patterns were performed using an X'PertPro PANalytical diffractometer, equipped with a Co Kα X-ray source ($\lambda = 1.789$ Å) and an X'celerator detector. The whole (2θ) angular region was scanned with steps of 0.0334°. Samples were placed on a flat holder and directly analyzed.

3. Results

3.1. Imaging: FE-SEM and AFM

Amine-derivatised cellulose films and fibres, after interaction with aqueous solution of $AgNO_3$ or $NaAuCl_4$ were observed by field emission scanning electron microscopy. Fig. 1(A) and (B) shows the modified cellulose films after interaction with the $AgNO_3$ for 15 and 45 min, respectively. In Fig. 1(C) and (D), one can see the resulting cellulose films after equivalent interactions with the $NaAuCl_4$ also for 15 and 45 min, respectively. All images show that the surfaces are highly and homogeneously covered with particles of very low dimensions. However, the size of the NPs depends on the contact times with the salt solutions. Indeed, as shown in Fig. 1(B) and (D), particles formed after 45 min of interaction with the salt solutions are clearly larger than those formed after 15 min (Fig. 1(A) and (C)), covering completely the cellulose surface. This suggests that, once the seed is generated, it starts to grow until reaching few tens of nanometres of nominal size, which is limited by lateral constrains. This hypothesis will be further supported by AFM imaging.

Fig. 2(A) and (B) shows amine-derivatised Avicel fibres after interaction with $AgNO_3$ and $NaAuCl_4$, respectively. In a general view, one can easily remark that films are smoother than the fibre samples. Here, in contrast, one can notice the presence of NPs with different sizes ranging from about 10 nm to 200 nm. Some of the larger particles reveal crystallographic shapes, essentially cubic forms in the case of silver or even octahedral, in the case of gold. This is coherent with the isometric system, where silver and gold crystallise (Dana & Ford, 1958). Fig. 2(C) shows an isolated Avicel fibre, where multiple nanocrystals also with cubic forms and larger dimensions (about 100 nm) are appended. This also lead us to believe that the removal of stereo constrains, stronger in compact

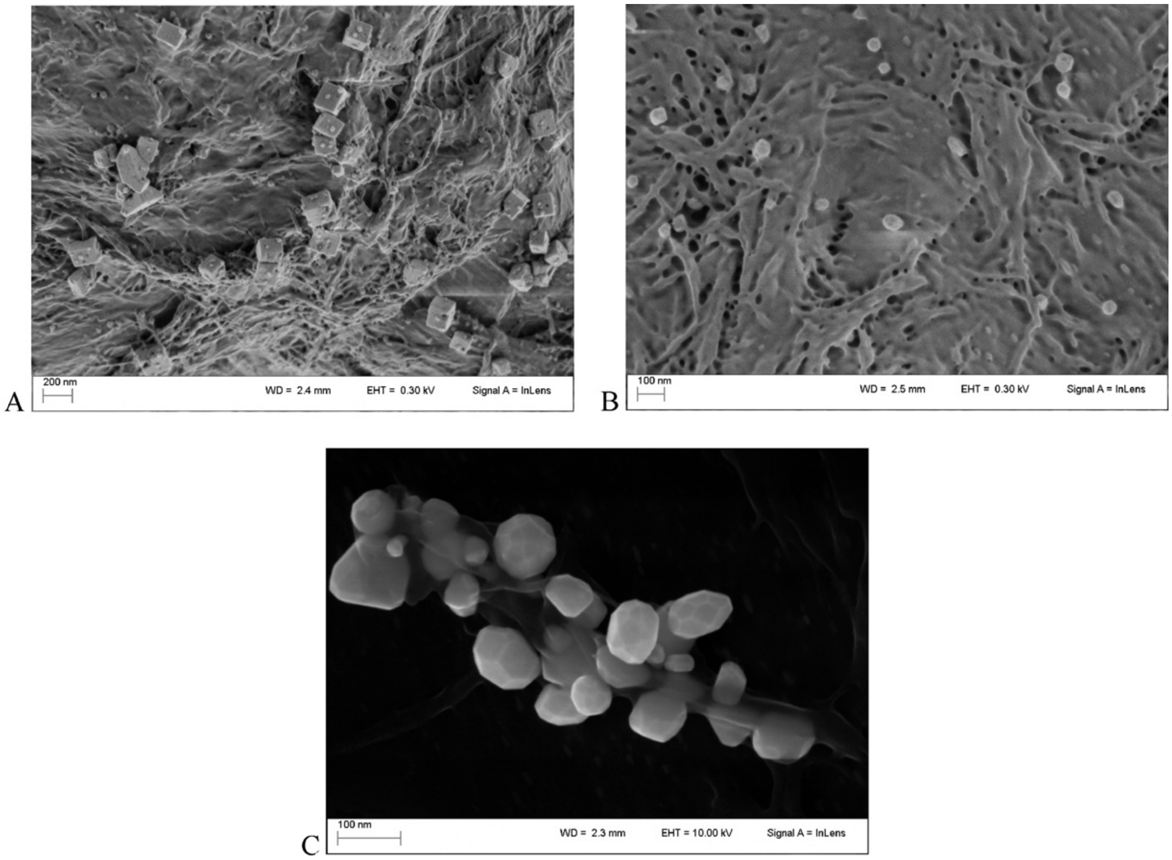

Fig. 2. FE-SEM images of: (A) amine-functionalised cellulose fibres after interaction with the AgNO3 solution for 15 min at room temperature; (B) cellulose fibres after interaction with the $NaAuCl_4$ solution for 30 min at 70 °C; (C) detail of an isolated fibre of the amine-functionalised cellulose fibres treated with the $NaAuCl_4$ solution.

films and less present in fibres, allows the development of crystals of higher dimensions, attaining more than 100 nm. However, it does not inhibit the growth of smaller NPs, as long as the chemical modification derivatisation of the surface with amine groups was performed.

Fig. 3 shows AFM images of cellulose surfaces after interaction with the $AgNO_3$ solution: an image of a non-modified cellulose surface after 60 min immersion is shown in (A). The other images show amine derivatised cellulose films immersed in the $AgNO_3$ solution for: (B) 15 min, (C) 30 min and (D) 45 min. Each image is accompanied of a depth scale. Besides the presence of the larger particles likely due to silver clusters, as it could be also visible above in the FE-SEM observations, on the non-modified cellulose image (A) only NPs, in low density, are observed on the non modified-cellulose film. Comparatively, the other images of amino-modified films clearly reveal higher densities of spherically shaped NPs packed on the surface, with diameters around 20 nm. After 15 min immersion (B), the particle size ranges from 10 to 15 nm and grows for longer contact times, attaining a size around 20 to 25 nm after 35 min immersion time (C). For 45 min (D), no obvious evolution is noticed, neither in the topography of film, nor in the NPs density and size, which seems to stabilise around 25 nm. No change in the AFM image was noticed as the films were submitted to thorough washing with deionised water and gentle sonication treatment; this favours the hypothesis of chemical bonding of the NPs to the surface. For both cellulose substrates, films or fibres, no evolution neither in the colour nor in the transparency of the solution was observed during the contact with $AgNO_3$ or $NaAuCl_4$ solution (for the fibres, the solution here referred, is the one recovered after centrifugation). One should emphasise again that the use of amine-modified cellulose substrate privileges a selective growth of NPs on the surface sites that were concerned with the chemical modification, preventing the generation of a continuous medium given the absence of a reducing agent.

3.2. XPS and UV/vis analyses

Many questions arise from these first observations concerning namely the chemical nature of the observed NPs, the selective character of their immobilisation on cellulose and eventually the occurrence of a covalent linkage to the surface and finally, the mechanisms that lead to the generation and growth of the NPs. To elucidate a part of these questions, further studies were carried on through UV/vis spectroscopy and XPS.

The prominent role of modified cellulose in the reduction process of Ag^+ can be emphasised through an experiment performed in homogenous conditions (liquid solution) to simulate those conditions under which the immobilisation process is carried on. For this purpose, a very dilute (10^{-4} M) aqueous solution of amine modified cellulose was used. Now, the modified cellulose becomes soluble as the amine grafting was carried out in homogenous solution allowing a very high substitution degree to be reached for the whole material and not only for the surface. The amine modified cellulose fibre was prepared following an activation procedure with CDI, as described in the experimental section. The addition of some drops of a 5×10^{-3} M solution of $AgNO_3$ to the colourless solution of amine derivatised cellulose provokes a gradual pink colour, becoming brownish after several hours, when visible particles settling down can be observed with naked eye. The time-dependent UV–vis absorption spectra, shown in Fig. 4, reveal a broad absorption band in the range of 350–430 nm, typical of the plasmon resonance band of Ag NPs (Kreibig & Genzel, 1985). The increasing intensity with

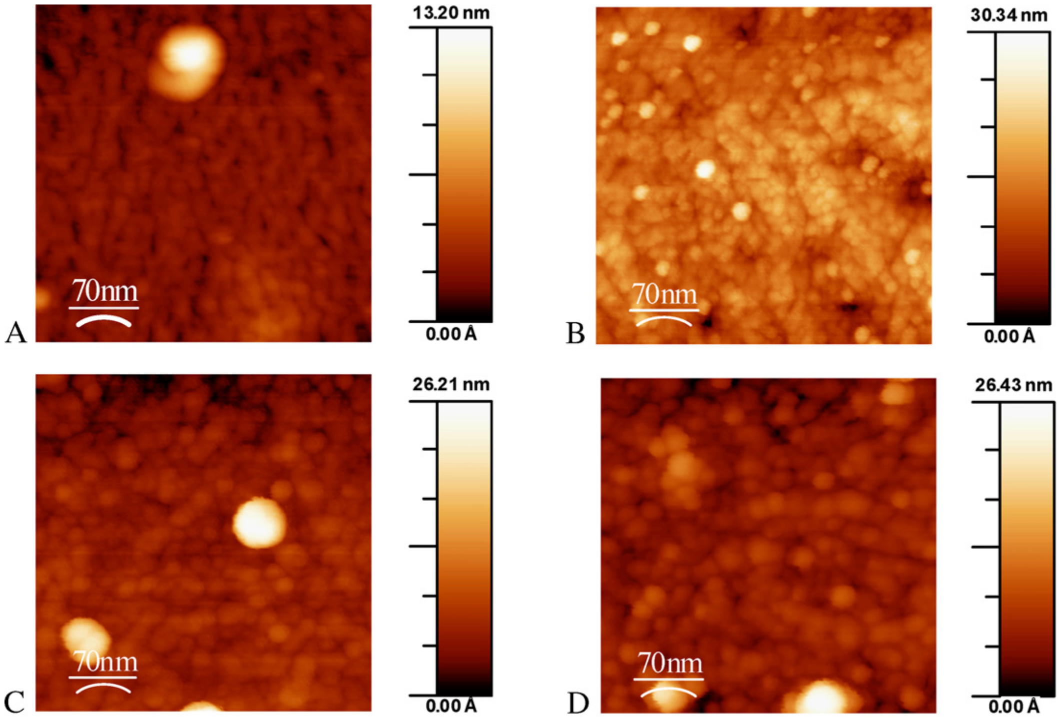

Fig. 3. AFM images of a non-modified cellulose film, deposited on GaAs, and immersed in the $AgNO_3$ solution for 60 min (A); amine-functionalised cellulose film immersed in the $AgNO_3$ solution for 15 min (B), amine-functionalised cellulose film immersed in the $AgNO_3$ solution for 30 min (C) and amine-functionalised cellulose film immersed in the $AgNO_3$ solution for 45 min (D). Each image is accompanied by a depth scale.

time of this band, tending to a limit after 30 min, indicates an increase of the Ag NPs concentration. Moreover, the plasmon band maximum gradually shifts from 370 nm to longer wavelengths, stabilizing around 390 nm after 30 min, pointing out an increase of the NPs size (Rogach, Shevchenko, Afanas, & Svidorov, 1997).

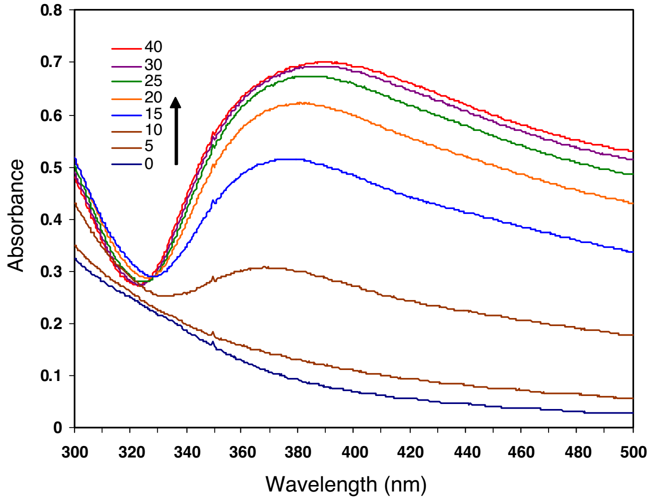

Fig. 4. Time-dependent UV–vis absorption spectra of a dilute aqueous solution of amine-functionalised cellulose prepared in water after the addition of some drops of a 5×10^{-3} M solution of $AgNO_3$.

In Fig. 5, XPS spectra of both the modified cellulose film (black points) and $AgNO_3$ powder (red points) are shown. The cellulose film was first functionalised with amine groups and doven in the $AgNO_3$ solution for 5 min, as described above, before being analyzed. N 1s region (Fig. 5(A)) presents two different contributions at 400.2 ± 0.1 and 402.3 ± 0.1 eV, assigned respectively to nitrogen from carbamate or free amine groups and N^+, likely due to NH_2 protonation. The presence of $AgNO_3$ on the surface can be discarded, since the contribution of N 1s from $AgNO_3$ centred at 407.2 ± 0.1 eV (red points) is absent in the spectrum of the cellulose film. In contrast, the presence of silver in the film is manifest. In fact, Ag 3d (Fig. 5(B)) is a doublet with an energy separation of 6.0 ± 0.1 eV. For the silver salt, Ag $3d_{5/2}$ is centred at 368.8 ± 0.1 eV, whereas after the interaction with the modified cellulose surface, this peak shifts to ~368.4 eV. Since the binding energies of metallic silver and silver oxides (Ag_2O and AgO) overlap (Wagner et al., 2003), the experimental Ag $3d_{5/2}$ peak may be assigned to silver in any one of its chemical states or can include contributions of all of them. On the other side, the Auger parameters (AP) for the same oxidation states are more distinctive and independent of the charge reference (Moretti, 2003). Therefore, for a detailed analysis of the nature of the detected silver in the cellulose film, we have studied the powdered oxides Ag_2O, AgO and a mechanical mixture of both, as well as a silver polished foil. The regions Ag MNN and Ag 3d were analyzed. The Auger parameters computed for the lines $Ag3d_{5/2}-M_5N_{45}N_{45}$ are 720.4, 717.9 and 718.4 eV for Ag^0, Ag^+ and Ag^{2+}, respectively. Ag 3d region for the cellulose modified film was, thence, fitted with the components corresponding to the findings for pure Ag, Ag_2O and AgO, in what concerns the asymmetric profile of the metallic silver and the distance between the binding energies of Ag_2O and AgO. The spin-orbit split was fixed to 6 eV. The fitting is shown in Fig. 5(B) for the modified cellulose film, yielding 41%, 47% and 12% (at.%) for Ag^0 (BE = 368.3 eV), Ag^+ (BE = 368.7 eV) and Ag^{2+} (BE = 368.0 eV), respectively. Thence, one can now estimate the weighted average AP, which is 719.0 eV. Experimentally, this can also be evaluated using the most intense $M_5N_{45}N_{45}$ Auger component (Fig. 5(C)) and the maximum of the Ag $3d_{5/2}$, leading to a value of 718.8 eV. This gives strength to the performed Ag 3d fitting even if the relative importance of the contributions are expected to be slightly different in photoelectron and Auger peaks, since their kinetic energies are quite different. This analysis proves undoubtedly that silver exists at the surface of the modified

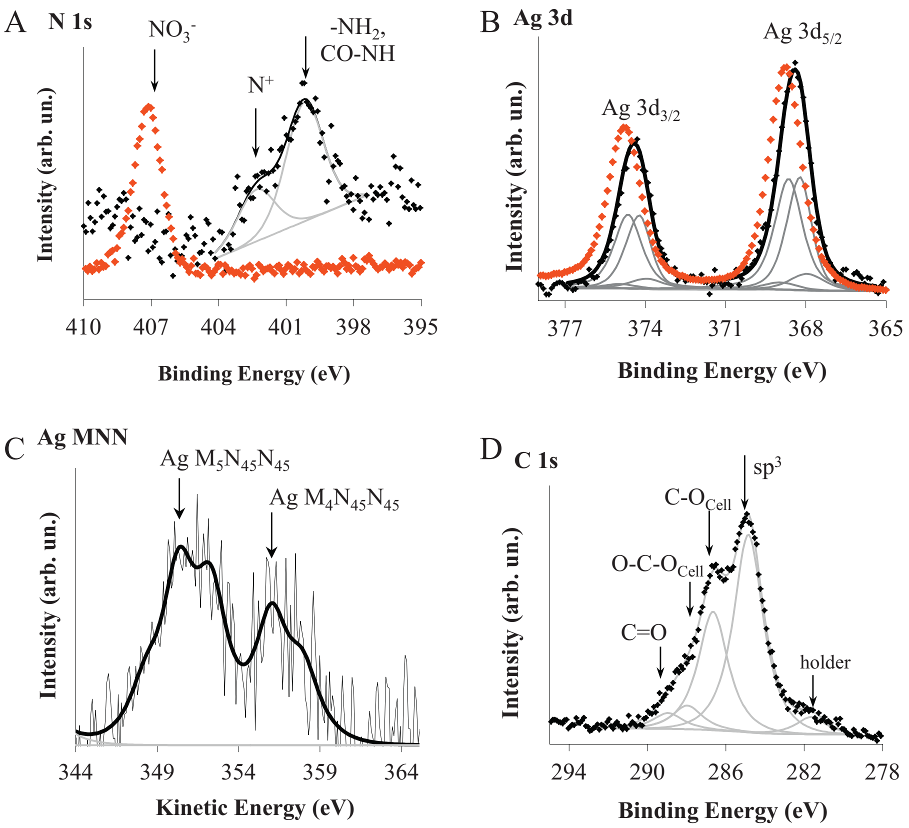

Fig. 5. XPS spectra of an amine-functionalised cellulose film on GaAs after interaction with AgNO$_3$ for 5 min (black points) and a sample of AgNO$_3$ (red points) showing different regions: (A) N 1s, (B) Ag 3d, (C) Ag MNN, (D) C 1s. (For interpretation of the references to color in this figure legend, the reader is referred to the web version of the article.)

cellulose film, and that besides metallic also oxidised silver is present. As a complementary information, one can observe that XPS C 1s region (Fig. 5(D)) includes the contribution of cellulose carbons centred at 286.7 and 288.0 ± 0.1 eV, aliphatic carbons from the amine alkyl chains, at 285 ± 0.1 eV and a component at 289.0 ± 0.1 eV assigned to a mixture of carbonyl, O–C=O (BE ∼ 289.0 eV), amide, N–C=O (BE ∼ 288.1 eV), and urethane, N(CO)O (BE ∼ 289.6 eV), groups.

Avicel cellulose fibres functionalised with amine groups and AgNO$_3$ or NaAuCl$_4$ were also characterised by XPS. Spectra of fibres treated with the silver salt also show that they are covered by a mixture of reduced and oxidised silver. Concerning fibres treated with NaAuCl$_4$, no Na is detected ruling out the presence of the initial salt. However, the analysis of Au 4f region (Fig. 6) is not very conclusive. Actually, the component Au 4f$_{7/2}$ at 85.2 ± 0.1 eV is far from the values reported in literature for metallic Au, which remain between 83.95 and 84.1 eV (Seah, 2001; Baer & Engelhard, 2010). Nevertheless, the Au 4f region can be fitted by a single asymmetric doublet, suggesting that gold is under the metallic form. The reported effect of the nanoparticle size on the increase of the binding energy only exists for smaller sizes than those here estimated for the gold nanoparticles (see below) (Baer & Engelhard, 2010). Anyway, for Au-nanoparticles on polyaniline, a nitrogen containing polymer, a maximum deviation of 0.4 eV was reported (Baer & Engelhard, 2010). In this case, the fact that we have primary amines and an insulating polymer may amplify the effect of the NPs size, and consequently, the energy deviation may reach a value around 1 eV, even for NPs larger than 10 nm. For instance, in Au@TiO$_2$ nanoparticles 10–15 nm sized, a binding energy negative shift of 0.9 eV was reported (Chen, Zhu, Yao, Wang, & Zhang, 2010). In what concerns the gold oxides, values reported in literature are all higher than the value found in our spectra (85.2 eV). These considerations combined with XRD results (see below) suggest that the Au NPs generated on modified cellulose are essentially composed by metallic gold.

3.3. XRD characterisation

The XRD was used to examine the crystal structure of metal nanoparticles and further identify the chemical structure of the different crystalline phases likely to be formed during the NPs growth. The XRD pattern, in the 15–60° 2θ range, for Avicel amine-

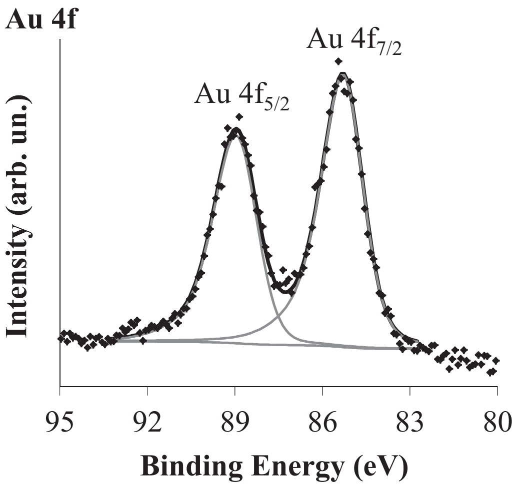

Fig. 6. Au 4f XPS region of an amine-functionalised cellulose fibres after interaction with the NaAuCl$_4$ solution at 70 °C.

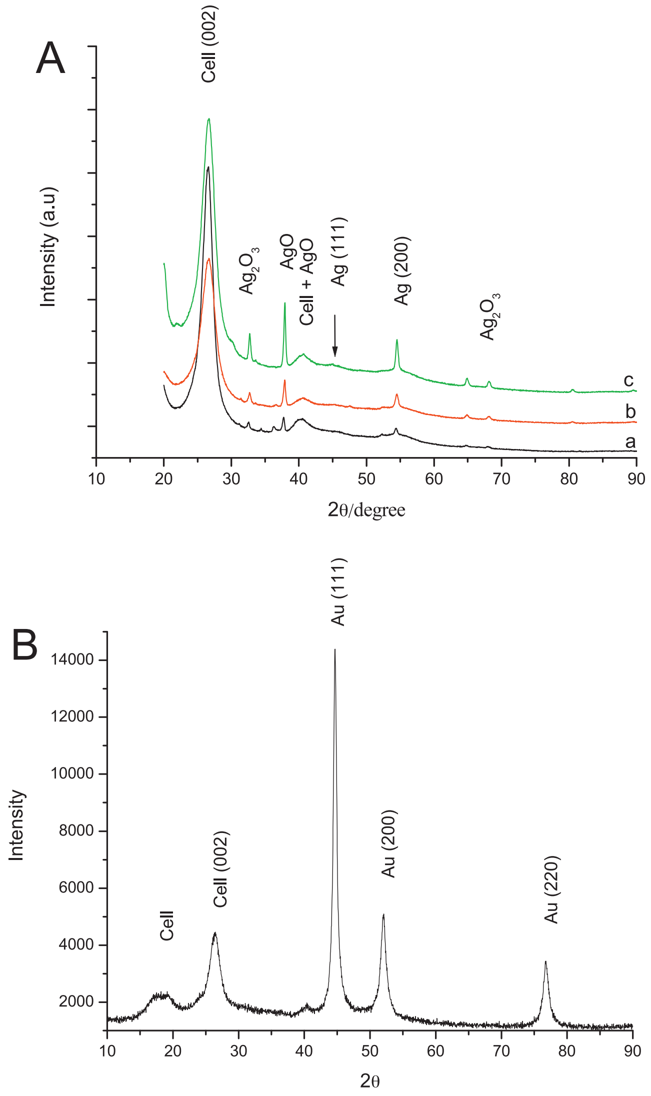

Fig. 7. XRD patterns of Avicel cellulose fibres: (A): non-modified fibres after 30 min of interaction with the AgNO$_3$ solution at room temperature (a), amine-functionalised fibres after 5 min interaction with the AgNO$_3$ solution at room temperature (b), amine-functionalised fibres after 35 min interaction with the AgNO$_3$ solution (c). (B) XRD pattern of amine-functionalised fibres after interaction with a NaAuCl$_4$ solution at 70 °C for 45 min.

functionalised cellulose fibres modified through the interaction with AgNO$_3$ or NaAuCl$_4$ aqueous solution are shown in Fig. 7(A) and (B), respectively. For both samples, characteristic peaks of cellulose I, arising at 18°, 26.6° and 40.4° (corresponding to 15°, 22° and 34°, if a Cu anticathode Cu Kα was used instead of the Co one) are assigned to the crystallographic planes (1 0 1), (0 0 2) and (0 4 0) (Garvey, Parker, & Simon, 2005). For AgNO$_3$ treated fibres, other diffraction peaks, appearing at 32.5°, 33.7° and a contribution at 34° (mixed with the cellulose one) can be ascribed to different crystalline silver oxide phases (AgO, Ag$_2$O and Ag$_2$O$_3$) (Waterhouse, Metson, & Bowmaker, 2007). In addition, other peaks located at 44.7° and 54.4° are a typical fingerprint of crystalline metallic Ag phase, corresponding to the crystallographic planes (2 2 0) and (2 0 0) (Kocareva, Grozdanov, & Pejova, 2001). On the other hand, in presence of NaAuCl$_4$, the diffraction peaks emanating from the NPs are essentially assigned to metallic Au phase with the characteristic peaks at 44.7°, 52° and 76.8°, attributed to the crystallographic planes (1 1 1), (2 0 0) and (2 2 0), respectively. On the other hand, one can estimate the mean particle size of NPs calculated from the value of the FWHM most intense peak, using Scherrer formula, which gives about 18 and 20 nm for Ag/AgO$_x$ and Au NPs, respectively.

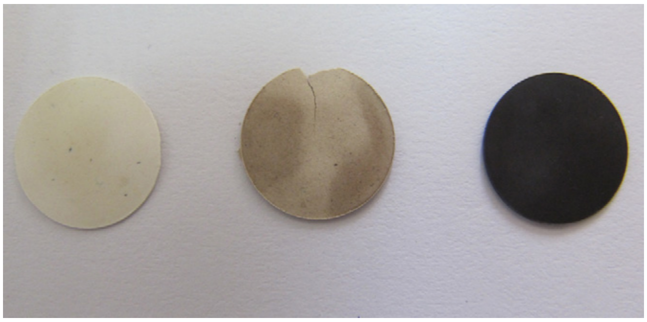

Fig. 8. Photography of three Avicel pellets: (A) raw cellulose fibres; (B) amine-functionalised fibres after interaction with the AgNO$_3$ solution at room temperature for 30 min; (C) amine-functionalised fibres after interaction with a NaAuCl$_4$ solution at 70 °C for 30 min.

4. Discussion

These values are in good agreement with those obtained from the microscopic analyses. It becomes also clear from XRD analysis that NPs are formed of silver and silver oxides, as the corresponding diffraction contributions are present in the XRD diagram. This completely agrees with XPS results, where a mixture of metallic ($\sim$2/5) and oxidised silver is detected. The oxidised species detected both by XPS and XRD may result from the oxidation (or hydroxylation) of silver in contact with the atmosphere to +1 and +2 oxidation states or from an incomplete reduction of the silver ions. The Ag NPs appear, then, to be made of a metallic core covered with silver hydroxide or oxide. For the non-derivatised sample (Fig. 7(A), curve (a)), the XRD pattern also exhibits the same peaks corresponding to silver but, comparatively to the amino-modified fibres, they are much less intense. This confirms, once again, the prominent role of the amine functionalisation of cellulose in favouring the growth of the Ag NPs. On the other hand, in the case of Au NPs, XPS results, despite confirming the presence of gold on the surface, are not very conclusive in what concerns its oxidation state.

Finally, we have checked if the method described above for generation of Ag NPs on cellulose films could be extended to other cellulosic surfaces either under the form of fibres or even to a sheet of paper. To approach this aspect, the same procedure for creation of Ag and Au NPs was applied to compacted pure cellulose fibres (Avicel), as it constitutes the main material of a paper sheet. As shown in Fig. 8, the colour of the pellets, change from white (original fibres) to yellow-brownish or deep purple after contacting with the AgNO$_3$ or the NaAuCl$_4$ solution, respectively. This is an indication of the presence of metal NPs on pellets, since the noticeable and different change of colour may be associated to the plasmon absorption of the Ag and Au nanoparticles.

Based on the above results, we propose a mechanism for selective Ag or Au NPs growth on modified cellulose as depicted in Scheme 2. The first step is the complexation of the metallic ions with the amine group or their sequestration by multiple amine groups, dangling from the modified cellulose surface. In a next step, the coordinated ions will be reduced by the hydroxyl groups of the anhydroglucosic unit of cellulose, giving rise to nuclei that will grow, fed by the diffusion of the metallic cations in the solution. The amino groups play a key role in the reduction of Ag or Au cations; on the one hand, the coordination between N and of Ag$^+$ (Frattini, Pellegri, Nicastro, & de Sanctis, 2005; Mishra, Sahu, Lim, Salamanca-Riba, & Bhattacharjee, 2010) and Au^{3+} (Chen et al., 2010), and on the other hand, the amino groups bring the precursor for the NPs generation in a close contact with the AGU, thus

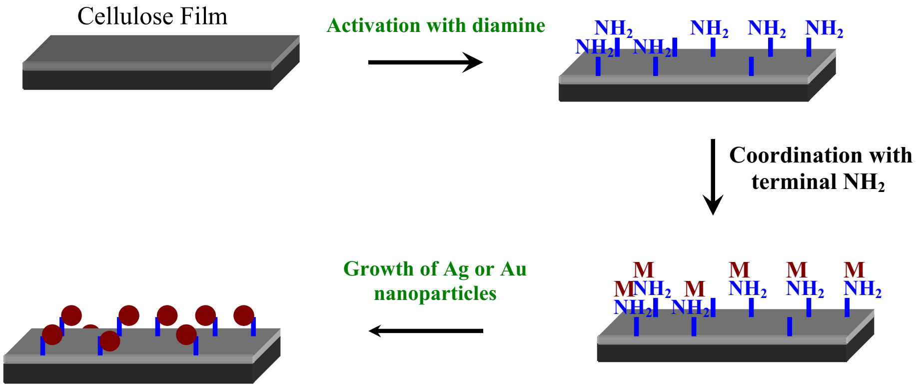

Scheme 2. Schematic illustration of the different steps in the generation of Ag or Au NPs.

promoting their reduction with the hydroxyl groups still existing in the cellulose unit. Thermodynamically, the redox reaction of a Ag^+ or $AuCl_4$—through the oxidation of an alcohol of AGU is possible, if we take into account that the Ox/red potential of ($RCOOH/RCH_2OH$) is in the range from 0.03 to 0.1 V and that of (Ag^+/Ag) and (Au^{3+}/Au) are 0.79 and 1.52 respectively. Actually, the redox potentials of the alcohols and the Ag^+ are compatible with the formation of Ag NPs. The reducing aptitude of the alcohol function and the oxidizing properties of Ag^+ are frequently reported in the literature. Thus, in the Fétizon oxidation (Fétizon & Golfier, 1968), Ag_2CO_3 is used as an oxidant for primary and secondary alcohols. The reduction of Ag^+ ions in 2-propanol, under basic pH, giving rise to metallic NPs, was investigated by Huang, Mills, & Hajek (1993). Silver NPs preparation, using different sugars (glucose, fructose), was also reported by Kvítek et al. (2005). Also, poly(ethylene glycol) was used as reducing agent for silver (Luo, Zhang, Zeng, Zeng, & Wang, 2005). One can assume that silver cations reduced by neighbouring hydroxyl groups are then dispersed on the surface sites, participating to the growth of the nanoparticle. If one takes into account that atomic radius of the silver atom is around 1.6 Å and the length of the AGU is of the order of 5 Å, and each of them contains two secondary alcohols and a primary one, one can expect that each AGU can host at the utmost three silver atoms.

However, one cannot exclude the possibility of the amino function to act both as a coordination site and as reducer. Indeed, polymeric amines containing primary, secondary and tertiary amino groups reacted over a period of several hours with $HAuCl_4$ giving rise to crystalline gold nanocrystals of 6–100 nm diameter. It has been postulated that the amino function acted as a dual reductant/stabiliser entity (Richardson, Johnston, & Borrmann, 2006). Also, the same dual role for the amino function in interaction with a silver salt solution was postulated by Kashiwagi, Yamamoto, & Nakamoto (2006). However these authors also pointed out a third role of the amino group as ligand of the intermediate silver complex.

One should emphasise here the fact that NPs are directly generated on cellulose surfaces bearing grafted amino groups, without any growth of NPs in the water solution. This is completely different from other approaches aiming to introduce Ag or other metallic NPs, previously formed in solution, on a cellulose substrate and, then, immobilised them by means of a physical interaction (Barud et al., 2008; Cai et al., 2009; Maria et al., 2009; Taylor et al., 2005). Actually, our approach opens the way toward a spontaneous generation of small NPs directly appended to cellulose substrates either in the form of films or fibres. Work is under progress to extend the method to cellulose whiskers and microfibrils, and concurrently, to other metallic precursors such as Cu, Pt, Fe and Ru. Furthermore, ongoing research is being carried in order to replace the step of the chemical modification by simply adding a water soluble polymer bearing amino groups, which is likely to adsorb in an irreversible way on cellulose fibres.

It is also worthy to note that our method assures the chemical immobilisation of the NPs nuclei on the grafted amine groups. Their immobilisation consequently decreases the risk of being leached off from the substrate, and allows stripping off the physisorbed ones, avoiding their agglomeration at the surface. Furthermore, the method contributes to favour the growth of NPs with a narrow size distribution, as it is clearly evident from the AFM observations.

5. Conclusions

The functionalisation of cellulose films and fibres, under mild conditions, with silver and gold NPs was developed. A prior chemical modification of the alcohol groups of the cellulose surface is needed for grafting amino functions, which will complex silver and gold ions. Therefore, NPs nucleation is only allowed and selectively accomplished on these seed coordination sites. The growth of NPs can be achieved by the interaction of aqueous dilute solutions of $AgNO_3$ or $NaAuCl_4$ with the cellulose substrate. The procedure limits the generation of NPs only to the cellulose surface, keeping the dispersion medium completely exempt of them. The resulting NPs are, consequently, chemically immobilised on the cellulose surface. This chemical anchoring of the NPs to the surface avoids particle desorption and extends the lifetimes of the resulting hybrid materials. Following this procedure, silver and gold NPs could be successfully created on cellulose and this was supported by field emission scanning electron microscopy (FE-SEM), atomic force microscopy (AFM), X-ray photoelectron spectroscopy (XPS) and XRD.

Observations show that the size of the particles increases with the time of interaction of the surfaces with the salt solution, attaining a constant value after 35 min. High NPs densities are confirmed by the FE-SEM and AFM observations. NPs average sizes tend to 25 nm, approximately. However, crystals several hundreds of nm-sized can be obtained specially in an isolated fibre, where less stereochemical constrains exist.

This is in good agreement with observations undertaken on very dilute aqueous solutions of amino-derivatised cellulose after adding some drops of an $AgNO_3$ solution. Here, the solution gradually turns from transparent to pink, becoming brownish after several hours. This evolution could be followed quantitatively using UV/vis spectroscopy. Here, the growth of the broad absorption band assigned to the silver plasmon observed between 350 and 430 nm and its gradual shift from 350 to 390 nm are associated to the increase of the NPs density and of their nominal size, respectively. These results are also compliant with those obtained from XPS and XRD that show the presence of silver and gold on the cellulose films and fibres. Moreover, in the case of silver, both techniques reveal the presence of different oxides, suggesting that NPs are composed by a mixture of metallic silver and silver oxides. In the case of gold, the presence of oxides is not patent from the experimental results, suggesting a predominant metallic character of the Au NPs.

The present study also shows that cellulose, pre-modified with amines, in interaction with aqueous solutions of silver or gold salts is a quite remarkable medium for an easy generation of Ag and Au NPs. The procedure could be extended to other systems. The changes of colour going from white, to pink and then to brown of the compacted solid Avicel fibres also suggest that the procedure can easily be applied to paper.

Acknowledgements

The authors gratefully recognise the financial support provided by NATO (grant NATO MD_CLG_982316). A.M.F. thanks Fundação para a Ciência e Tecnologia for postdoctoral grant, SFRH/BPD/26239/2006. S.B. and A.M.B.R. thank the Scientific and Technological Cooperation Portugal/Tunisia (no. 441.00 Tunisia and 46/TP/09).

References

Agrawal, M., Pich, A., Zafeiropoulos, N. E., Gupta, S., Pionteck, J., Simon, F., et al. (2007). Polystyrene-ZnO composite particles with controlled morphology. *Chemistry of Materials*, *19*, 1845–1852.

Agrawal, M., Pich, A., Zafeiropoulos, N. E., & Stamm, M. (2008). Fabrication of hollow titania microspheres with tailored shell thickness. *Colloid & Polymer Science*, *286*, 593–601.

Alila, S., Ferraria, A. M., Botelho do Rego, A. M., & Boufi, S. (2010). Controlled surface modification of cellulose fibres by amino derivatives using N,N′-carbonyldiimidazole as activator. *Carbohydrate Polymers*, *77*, 553–562.

Baer, D. R., & Engelhard, M. H. (2010). XPS analysis of nanostructured materials and biological surfaces. *Journal of Electron Spectroscopies and Related Phenomena*, *178*, 415–432.

Barud, H. S., Barrios, C., Regiani, T., Marques, R. F. C., Verelst, M., Dexpert-Ghys, J., et al. (2008). Self-supported silver nanoparticles containing bacterial cellulose membranes. *Materials Science & Engineering C: Biomimetic and Supramolecular Systems*, *28*, 515–518.

Benaissi, K., Johnson, L., Walsh, D. A., & Thielemans, W. (2010). Synthesis of platinum nanoparticles using cellulosic reducing agents. *Green Chemistry*, *12*, 220–222.

Boufi, S., Rei Vilar, M., Parra, V., Ferraria, A. M., & Botelho do Rego, A. M. (2008). Grafting of porphyrins on cellulose nanometric films. *Langmuir*, *24*, 7309–7315.

Cai, J., Kimura, S., Wada, M., & Kuga, S. (2009). Nanoporous cellulose as metal nanoparticles support. *Biomacromolecules*, *10*, 87–94.

Campbell, C. T., Parker, S. C., & Starr, D. E. (2002). The effect of size-dependent nanoparticle energetics on catalyst sintering. *Science*, *298*, 811–814.

Chen, J., Wang, J., Zhang, X., & Jin, Y. (2008). Microwave-assisted green synthesis of silver nanoparticles by carboxymethyl cellulose sodium and silver nitrate. *Materials Chemistry & Physics*, *108*, 421–424.

Chen, Y. L., Zhu, B. L., Yao, M. Y., Wang, S. R., & Zhang, S. M. (2010). The preparation and characterization of Au@TiO_2 nanoparticles and their catalytic activity for CO oxidation. *Catalysis Communications*, *11*, 1003–1007.

Daniel, M. C., & Astruc, D. (2004). Gold nanoparticles: Assembly, supramolecular chemistry, quantum-size-related properties, and applications toward biology, catalysis, and nanotechnology. *Chemical Reviews*, *104*, 293–346.

Dana, E. S., & Ford, W. E. (1958). *A textbook of mineralogy* (4th ed.). New York: John Wiley and Sons Inc.

Esumi, K., Isono, R., & Yoshimura, T. (2004). Preparation of PAMAM- and PPI-metal (silver, platinum, and palladium) nanocomposites and their catalytic activities for reduction of 4-nitrophenol. *Langmuir*, *20*, 237–243.

Ferraria, A. M., Boufi, S., Battaglini, N., Botelho do Rego, A. M., & Vilar, M. R. (2010). Hybrid systems of silver nanoparticles generated on cellulose surfaces. *Langmuir*, *26*, 1996–2001.

Ferraria, A. M., Lopes da Silva, J. D., & Botelho do Rego, A. M. (2003). XPS studies of directly fluorinated HDPE: Problems and solutions. *Polymer*, *44*, 7241–7249.

Fétizon, M., & Golfier, M. (1968). Selective oxidation of alcohols by silver carbonate. *Comptes Rendus Hebdomadaires des Séances de l'Académie des Sciences (C)*, *267*, 900–903.

Frattini, A., Pellegri, N., Nicastro, D., & de Sanctis, O. (2005). Effect of amine groups in the synthesis of Ag nanoparticles using aminosilanes. *Materials Chemistry & Physics*, *94*, 148–152.

Garvey, C. J., Parker, I. H., & Simon, G. P. (2005). On the interpretation of X-ray diffraction powder patterns in terms of the nanostructure of cellulose I fibres. *Macromolecular Chemistry & Physics*, *206*, 1568–1575.

He, J. H., Kunitake, T., & Nakao, A. (2003). Facile in situ synthesis of noble metal nanoparticles in porous cellulose fibers. *Chemistry of Materials*, *15*, 4401–4406.

Horcas, I., Fernandez, R., Gomez-Rodriguez, J. M., Colchero, J., Gomez-Herrero, J., & Baro, A. M. (2007). WSXM: A software for scanning probe microscopy and a tool for nanotechnology. *Review of Scientific Instruments*, *78*, 1–8.

Huang, Z. Y., Mills, G., & Hajek, B. (1993). Spontaneous formation of silver particles in basic 2-propanol. *Journal of Physical Chemistry*, *97*, 11542–11550.

Kashiwagi, Y., Yamamoto, M., & Nakamoto, M. (2006). Facile size-regulated synthesis of silver nanoparticles by controlled thermolysis of silver alkylcarboxylates in the presence of alkylamines with different chain lengths. *Journal of Colloid & Interface Science*, *300*, 169–175.

Kocareva, T., Grozdanov, I., & Pejova, B. (2001). Ag and AgO thin film formation in Ag^+-triethanolamine solutions. *Materials Letters*, *47*, 319–323.

Kreibig, U., & Genzel, L. (1985). Optical-absorption of small metallic particles. *Surface Science*, *156*, 678–700.

Kvítek, L., Prucek, R., Panáček, A., Novotny, R., Hrbáč, J., & Zbořril, R. (2005). The influence of complexing agent concentration on particle size in the process of SERS active silver colloid synthesis. *Journal of Materials Chemistry*, *15*, 1099–1105.

Luo, C. C., Zhang, Y. H., Zeng, X. W., Zeng, Y. W., & Wang, Y. G. (2005). The role of poly(ethylene glycol) in the formation of silver nanoparticles. *Journal of Colloid & Interface Science*, *288*, 444–448.

Maier, S. A., Brongersma, M. L., Kik, P. G., Meltzer, S., Requicha, A. A. G., & Atwater, H. A. (2001). Plasmonics – A route to nanoscale optical devices. *Advanced Materials*, *13*, 1501–1505.

Malynych, S., Luzinov, I., & Chumanov, G. (2002). Poly(vinyl pyridine) as a universal surface modifier for immobilization of nanoparticles. *Journal of Physical Chemistry B*, *106*, 1280–1285.

Maria, L. C. D., Santos, A. L. C., Oliveira, P. C., Barud, H. S., Messaddeq, Y., & Ribeiro, S. J. L. (2009). Synthesis and characterization of silver nanoparticles impregnated into bacterial cellulose. *Materials Letters*, *63*, 797–799.

Mishra, T., Sahu, R. K., Lim, S. H., Salamanca-Riba, L. G., & Bhattacharjee, S. (2010). Hexadecylamine capped silver and gold nanoparticles: Comparative study on formation and self-organization. *Materials Chemistry & Physics*, *123*, 540–545.

Moretti, G. (2003). The Auger parameter. In D. Briggs, & J. T. Grant (Eds.), *Surface analysis by Auger and X-ray photoelectron spectroscopy* (pp. 501–530). Trowbridge: IM Publications and Surface Spectra Lim.

Pich, A., Hain, J., Lu, Y., Boyko, V., Prots, Y., & Adler, H.-J. (2005). Hybrid microgels with ZnS inclusions. *Macromolecules*, *38*, 6610–6619.

Richardson, M. J., Johnston, J. H., & Borrmann, T. (2006). Monomeric and polymeric amines as dual reductants/stabilisers for the synthesis of gold nanocrystals: A mechanistic study. *European Journal of Inorganic Chemistry*, *13*, 2618–2623.

Rogach, A. L., Shevchenko, G. P., Afanas, Z. M., & Svidorov, V. V. (1997). Changes in the morphology and optical absorption of colloidal silver reduced with formic acid in the polymer matrix under UV irradiation. *Journal of Physical Chemistry B*, *101*, 8129–8132.

Rubio-Retama, J., Zafeiropoulos, N. E., Serafinelli, C., Rojas-Reyna, R., Voit, B., Cabarcos, E. L., et al. (2007). Synthesis and characterization of thermosensitive PNIPAM microgels covered with superparamagnetic gamma-Fe_2O_3 nanoparticles. *Langmuir*, *23*, 10280–10285.

Scott, R. W. J., Wilson, O. M., & Crooks, R. M. (2005). Synthesis, characterization, and applications of dendrimer-encapsulated nanoparticles. *Journal of Physical Chemistry B*, *109*, 692–704.

Seah, M. P. (2001). Summary of ISO/TC 201 Standard: VII ISO 15472: 2001—surface chemical analysis—X-ray photoelectron spectrometers—calibration of energy scales. *Surface & Interface Analysis*, *31*, 721–723.

Sperling, R. A., Gil, P. R., Zhang, F., Zanella, M., & Parak, W. J. (2008). Biological applications of gold nanoparticles. *Chemical Society Reviews*, *37*, 1896–1908.

Tankhiwale, R., & Bajpai, S. K. (2009). Graft copolymerization onto cellulose-based filter paper and its further development as silver nanoparticles loaded antibacterial food-packaging material. *Colloid Surface B: Biointerfaces*, *69*, 164–168.

Taylor, P. L., Ussher, A. L., & Burrel, R. E. (2005). Impact of heat on nanocrystalline silver dressings. Part I: Chemical and biological properties. *Biomaterials*, *26*, 7221–7229.

Vainio, U., Pirkkalainen, K., Kisko, K., Goerigk, G., Kotelnikova, N. E., & Serimaa, R. (2007). Copper and copper oxide nanoparticles in a cellulose support studied using anomalous small-angle X-ray scattering. *The European Physical Journal D*, *42*, 93–101.

Vilar, M. R., Boufi, S., Ferraria, A. M., & Botelho do Rego, A. M. (2007). Chemical modification of semiconductor surfaces by means of nanometric cellulose films. *Journal of Physical Chemistry C*, *111*, 12792–12803.

Wagner, C. D., Naumkin, A. V., Kraut-Vass, A., Allison, J. W., Powell, C. J., & Rumble, J. R., Jr. (2003). *NIST X-ray photoelectron spectroscopy database, standard reference database 20, version 3.5*. National Institute of Standards and Technology (NIST). [accessed April 15, 2011]

Waterhouse, G. I. N., Metson, J. B., & Bowmaker, G. A. (2007). Synthesis, vibrational spectra and thermal stability of Ag_3O_4 and related Ag_7O_8X salts ($X = NO_3^-$ ClO_4^-, HSO_4^-). *Polyhedron*, *6*, 3310–3322.

Wu, M., Kuga, S., & Huang, Y. (2008). Quasi-one-dimensional arrangement of silver nanoparticles templated by cellulose microfibrils. *Langmuir*, *24*, 10494–10497.